Nano Trends 13 (2026) 100178

Contents lists available at ScienceDirect

Nano Trends

journal homepage: www.elsevier.com/locate/nantre

Measurement of charge carrier mobilities in thin films via the space-charge limited current (SCLC) method; A practical example

Marzieh Rabiei [a,*], Sohrab Nasiri [a,b,*], Juozas Padgurskas [a], Raimundas Rukuiza [a]

[a] Department of Mechanical, Energy and Biotechnology Engineering, Faculty of Engineering, Vytautas Magnus University, Akademija, LT-53361, Kauno r, Lithuania
[b] Faculty of Mechanical Engineering and Design, Kaunas University of Technology, Studentu Street 56, Kaunas, LT 51373, Lithuania

ARTICLE INFO

Keywords:
Charge mobility
Hole-only device
Electron-only device
Mott-Gurney
SCLC

ABSTRACT

Study of space charge limited current (SCLC) transport in charge carrier injection is presented. It is shown that the accurate and convenient calculation of carrier mobility, which has been neglected in many previous studies on transport in optical and electrical devices, is essential to obtain physically meaningful spatial carrier densities and field distributions. In this work, the SCLC technique to accurately determine the mobility of holes and electrons in organic semiconductors is investigated in detail. Recognizing the importance of balanced charge transport to the performance of optical and electronic devices, the fundamentals of SCLC, including Mott-Gurney's law, are discussed and its advantages over alternative methods are highlighted. A carbazole-based compound is used as a practical example, with single-carrier devices fabricated to selectively measure hole-only and electron-only transport. The current-voltage characteristics were analysed in the trap-free SCLC regime (slope ≈ 2 in log-log plots), and yielded mobilities of $\mu_e = 4.02 \times 10^{-5}$ $cm^2V^{-1}s^{-1}$ and $\mu_h = 1.84 \times 10^{-3}$ $cm^2V^{-1}s^{-1}$. This study not only demonstrates a clear and reproducible method for mobility extraction, but also highlights the importance of SCLC measurements under device-like conditions for material selection and performance optimization in optoelectronic applications.

1. Introduction

The importance of the mobility of electrons and holes and even the realization that there might be differences, emerged in early semiconductor physics in the mid-20th century, as researchers tried to explain why certain devices worked better or worse. In the 1940s-1950s, during the development of the first germanium and silicon transistors, scientists such as Shockley, Bardeen, and Brattain measured carrier drift and diffusion [1–3]. They found that the current-voltage behaviour strongly depends on how fast electrons or holes can move through the crystal. Mobility was initially determined using Hall effect measurements, in which the researchers were able to calculate the drift velocity per unit electric field for electrons and holes separately by applying a magnetic field [4]. Today, charge carrier mobility is considered a fundamental material property, just like the band gap or the absorption spectrum. It is measured in almost every semiconductor study because it predicts how fast charges can get to where they are needed. It determines the power efficiency and the reaction time. Without knowledge of charge carrier mobility, it is almost impossible to develop powerful and stable optical and electrical devices, as it is not possible to predict or control how charges behave inside materials [5]. The mobility of holes and electrons describes how easily each type of charge carrier moves through a material when an electric field is applied. Electron mobility (μ_e) is the measure of how fast electrons can drift through the conduction band of a semiconductor. Furthermore, hole mobility (μ_h) is the measure of how fast holes (which effectively represent the absence of electrons in the valence band) can move through the material [6,7]. They are both defined as, $\mu = \frac{\vartheta_d}{E}$, which μ is the mobility ($cm^2V^{-1}s^{-1}$), ϑ_d is the drift velocity of the carrier (cms^{-1}) and E is the applied electric field (Vcm^{-1}) respectively. In most organic semiconductors, the mobilities of electrons and holes are not equal, often one of them is much lower, resulting in unbalanced transport. High mobility also means that the charge carriers can move quickly and with less scattering or trapping, which improves the efficiency of the devices [7,8]. There are two known techniques for measuring charge carrier mobility: 1) space charge limited current (SCLC) and 2) time of flight (TOF) [9,10]. Whether SCLC or TOF, is the better-known technique depends on the research context, but in modern organic electronics, e.g., light-emitting diodes (LEDs), organic light-emitting diodes (OLEDs), and perovskite devices, SCLC is

* Corresponding authors.
E-mail addresses: rabieimarzieh7@gmail.com (M. Rabiei), sohrab.nasiri2017@gmail.com (S. Nasiri).

https://doi.org/10.1016/j.nwnano.2025.100178
Received 14 October 2025; Received in revised form 17 December 2025; Accepted 20 December 2025
Available online 20 December 2025

increasingly used and cited because it is easier to implement, works well for thin films, and requires only simple current-voltage measurements without specialized laser equipment [11]. While TOF, is the classic method in semiconductor physics and still valuable for studying thick films and bulk transport properties, it is less commonly used in current thin film device research, making SCLC the better choice today. SCLC is a steady-state electrical method in which a voltage is applied to a single carrier device, and the current-voltage (J-V) characteristics in the space-charge regime are analysed using Mott-Gurney's law. It is well suited for thin films (typically 50–500 nm) and device-like structures, requires only simple electrical measurements, and is commonly used in organic optoelectronics to extract either hole or electron mobility by contact matching. However, SCLC generally provides an effective mobility that reflects trap effects and dependencies on operating- conditions rather than an intrinsic transit time [12–15]. In contrast, TOF is a transient optical-electrical technique in which a short pulse of light generates charge carriers at one electrode, and their drift to the opposite electrode is monitored under an applied bias voltage. The transit time of the charge carriers is measured directly from the transient photocurrent, so that the mobility can be derived from the layer thickness, the applied voltage, and the drift time. TOF is better suited for thicker films (often >1 μm), can measure electron and hole mobility separately by reversing polarity, and provides more information about intrinsic transport, but requires specialized pulsed light sources and fast detection electronics [16,17]. In short, SCLC is simpler, instrument-friendly, and widely used in modern organic thin film devices, while TOF is more directly suitable for determining intrinsic mobility in thicker samples, but is experimentally more challenging. The SCLC method is experimentally straightforward and inexpensive, requiring only a single-carrier device and standard current-voltage measurements, without the need for complex laser setups or high-speed electronics. It is well suited for very thin films (tens to hundreds of nanometers), which match the active layer thickness of most optical devices. By using selective electrodes, it enables the separate measurement of hole and electron mobilities within the same material. In addition, SCLC determines mobility under realistic device-like conditions, ensuring that the extracted values are directly relevant to operational performance. The technique can also reveal trapping effects by examining deviations from the ideal Mott-Gurney law, providing valuable insight into material purity and defect states [18]. A clear explanation of the mobility calculation is essential for transparency, reproducibility, and accurate comparison with other studies, while a practical example helps to demonstrate the application of the method and guide the reader in obtaining reliable results. This study is intended as a tutorial or methodological guide, and the presented findings serve as illustrative examples rather than benchmarks aimed at establishing new material performance records. The reported mobility values are presented with limited significant figures and are intended as illustrative examples, as a detailed analysis of measurement uncertainties is beyond the scope of this tutorial. In view of the lack of a clear explanation in the calculation of mobility and recognizing the importance of hole and electron mobility values for selecting materials in optical and electrical devices, in this study, we present an in-depth discussion of the SCLC technique, along with a practical example demonstrating the precise calculation of hole and electron mobilities.

2. Materials and instrumentation

The chemical components and solvents were provided in analytical grade and used without further purification. All measurements were performed in an air atmosphere. All measurements were performed at room temperature (22–25 °C) under ambient laboratory air, not in a glovebox. The relative humidity during measurements was approximately 40–55 %. No inert-gas atmosphere was used because the purpose of this work was to demonstrate the SCLC mobility-extraction procedure, rather than to benchmark absolute device performance. The current-voltage-luminance characteristics were checked with Keithley 2400 SourceMeter SMU, Ocean Optic Instruments and Mastech-MS6612 Optical Meter, respectively. The film thickness was 200 nm. The physical vapor deposition (PVD) deposition rate was 3 Å/s, the annealing temperature was 120 °C, THF was used as the solvent, and the device pixel area was 3 × 3 mm.

3. Results and discussion

3.1. Mott-Gurney law

The Mott-Gurney law describes space-charge-limited current under trap-free conditions with constant carrier mobility, derived from Poisson's equation and current continuity. It was first developed by N.F. Mott and R.W. Gurney in the 1940s when studying electron injection in insulating crystals and later became a standard model for organic semiconductors [19–21]. The calculation of Mott-Gurney's law can be based on two important physical laws; the poisson equation (relates the electric field (E) to the charge density (ρ)) (Eq. (1)) [22]:

$$\frac{dE}{dx} = \frac{\rho}{\varepsilon} \tag{1}$$

In this equation, ρ=qp(x) for holes (or qn(x) for electrons) and it is Gauss's law in one-dimensional differential form for the electric field (E), where ρ is the space charge density (Cm^{-3}), ε is the dielectric constant of the material and x is the position coordinate. Within the SCLC model, the extracted mobility is inversely proportional to ε_r; therefore, assuming a higher dielectric constant results in a proportionally lower calculated mobility, while a lower ε_r leads to a higher extracted mobility. Since ε_r typically varies within a narrow range for organic materials, this mainly causes a systematic scaling of mobility without affecting the overall transport trends. In addition, for holes in semiconductors, ρ(x)=q p(x), where q is the elementary charge (1.602×10^{-19C}) and p(x) is the hole concentration (m^{-3}). Furthermore, for electrons ρ(x)=q n(x), where n(x) is the electron concentration (m^{-3}) [23]. If Gauss's law is combined with the drift current equation to establish the SCLC derivation, the drift current-only equation for holes (Eq. (2)) is [24],

$$J = qp(x)\mu E(x) \tag{2}$$

Where J is the current density (Am^{-2}), which is constant in the steady state, and μ is the mobility of the holes ($m^2V^{-1}s^{-1}$) [25].

By inserting of $p(x) = \frac{J}{q\mu E(x)}$ into Gauss' law, Eq. (3) can be set up,

$$\frac{dE}{dx} = \frac{q}{\varepsilon}\frac{J}{q\mu E(x)} = \frac{J}{\varepsilon\mu E(x)} \tag{3}$$

This is the differential equation that links the spatial change of E with E itself in the case of pure drift current-only conduction. When integrating the electric field profile with multiplication of both sides and separation by E (x), Eq. (4) was established.

$$E(x)\frac{dE}{dx} = \frac{J}{\varepsilon\mu} \tag{4}$$

With integrate once (Eq. (5));

$$\int E\frac{dE}{dx}dx = \int \frac{J}{\varepsilon\mu}dx \tag{5}$$

On the left, E $\frac{dE}{dx}$ integrates to $\frac{E^2}{2}, \frac{E^2}{2} = \frac{J}{\varepsilon\mu}\, x + C$

If we apply the boundary condition and assume $E = 0$ at $x = 0$, the result is $C = 0$ and thus Eq. (6);

$$\frac{E^2}{2} = \frac{J}{\varepsilon\mu}\, x \tag{6}$$

So, the Eq. (6) can be written, $E = \sqrt{\frac{2Jx}{\varepsilon\mu}}$

Based on the definition of the electrostatic potential based on the

applied voltage (V), the electric field in electrostatics is also the negative gradient of the potential in Eq. (7);

$$E(x) = -\frac{dV}{dx} \tag{7}$$

Convert to E(x) dx=−dV and integrate from $x = 0$ (one electrode) to $x = d$ (the other):

$$\int_0^d E(x)\,dx = -\int_{V(0)}^{V(d)} dV = V(0) - V(d)$$

The applied voltage is the potential difference between the electrodes, Eq. (8),

V(applied)=V(0)-V(d), therefore,

$$V(applied) = \int_0^d E(x)\,dx \tag{8}$$

With the substitution $E=\sqrt{\frac{2Jx}{\varepsilon\mu}}$ in Eqs. (8), Eq. (9) can be considered;

$$V(applied) = \int_0^d E(x)\,dx = \int_0^d \sqrt{\frac{2J}{\varepsilon\mu}}x^{1/2}dx = \sqrt{\frac{2J}{\varepsilon\mu}}\,\frac{2}{3}\,d^{3/2} \tag{9}$$

Solve for J:

$\left(\frac{3V}{2}\right)^2 = \frac{2J}{\varepsilon\mu}d^3 \rightarrow J=\frac{9}{8}\varepsilon\mu\frac{V^2}{d^3}$, Mott-Gurney law Eq. (10) can be gained.

$$J = \frac{9}{8}\,\varepsilon\mu\,\frac{V^2}{d^3} \tag{10}$$

3.2. SCLC technique in practical aspect

To apply the Mott-Gurney relation $J=\frac{9}{8}\varepsilon_r\varepsilon_0\mu\frac{V^2}{d^3}$, it should be first designing a single-carrier diode that conducts only holes or only electrons. This means that it can be selected by contacts that are ohmic for the desired charge carrier and block for the opposite type (e.g., ITO/ 4,4′-Cyclohexylidenebis[N,N-bis(4-methylphenyl)benzenamine] (TAPC)/ as the connection for calculating the mobility/TAPC/Al for holes; ITO/ 1,3,5-Tri(m-pyridin-3-ylphenyl)benzene, 1,3,5-Tris(3-pyridyl-3-phenyl)benzene, (TmPyPB)/ as the connection for calculating the mobility /TmPyPB/LiF/Al for electrons) [26,27]. Keep the active layer uniform and measure its thickness d accurately. Confirm the device area, then record a stable J-V sweep from low to higher voltage to avoid transients, and plot the data as log J versus log V. At low voltage, it can be seen an Ohmic region with a slope of ~ 1; when the injected carriers dominate, the curve bends into a region with a slope of ~ 2, the trap-free SCLC window where Mott-Gurney applies. Use data points from this segment with slope ~ 2, and if material has a non-negligible built-in voltage V_{bi}, replace V with $V-V_{bi}$. Insert the dielectric constant ε_r (from literature or measured) and d, then mobility μ can be solved. It is usual to use the whole slope ~ 2 and not just a single point, rearrange to $\frac{Jd^3}{V^2} = \frac{9}{8}\varepsilon\mu$ and fit a straight line versus nothing (i.e., take the mean) or equivalently fit J vs V with d fixed [28]. If the slope is greater than 2, it is a trap-limited SCLC. In this case, Mott-Gurney underestimates the complexity; either extract a trap-filled limiting stress to estimate the trap density, or use an exponential trap or Gaussian DOS model. If the slope varies between 1 and 2, check for contact injection barriers, leakage or field-dependent mobility; the classical equation assumes constant μ and negligible diffusion [29,14]. A few practical hints are helpful: verify symmetric forward/backward scans to rule out hysteresis, keep compliance limits high enough to reach the SCLC regime without hitting series resistance, and avoid Joule heating, mobility drifts with temperature. Finally, provide μ with the assumptions you used (trap-free vs trap-limited V_{bi} correction, ε_r source) so that others can reproduce your extraction. In SCLC analysis, plotting log J vs log V is mainly a tool to show the power law relationship between current and voltage in a clear, quantitative way. When the SCLC model is valid, the current follows a relationship of the form $J \propto V^m$, where m is the slope in a log-log plot. For SCLC without traps, the theory predicts $m \approx 2$ [13]. The typical current-voltage scaling of SCLC regions is shown in Fig. 1. If the plot J versus V directly on linear axes, it can see the curvature, but it is much harder to identify exactly where the dependence changes from ohmic ($m \approx 1$) to SCLC ($m \approx 2$) or to trap-limited ($m > 2$). Linear plots also compress the low-voltage region and exaggerate the high-voltage region, making the transitions less obvious. Take the logarithms of both axes, log $J = m$ log V+constant, the slope m becomes a simple visual indicator of the conductivity range [30]. A slope of 1 indicates resistive conduction, 2 indicates trap-free SCLC, and higher slopes indicate trap-limited behaviour. This log-log approach also works over several orders of magnitude of current and voltage, which is common in organic semiconductors [31,32]. Using log-log not because the physics is logarithmic, the underlying law is still quadratic, but because the logarithmic scaling makes it straightforward to pinpoint the regime and extract the exponent mmm without ambiguity. If the material is free of traps and the injected charge carriers dominate over the thermally generated charge carriers, the Poisson equation and the drift current Eq. (11) combine;

$$J = \frac{9}{8}\,\varepsilon_r\varepsilon_0\mu\,\frac{V^2}{d^3} \tag{11}$$

This relationship states that J is proportional to V^2. If the slope is exactly 2, this mean that the trap-free SCLC regime can be announced. If the curve shows a clear kink in the trap-filled-limit (TFL) curve, it can treat anything above this kink as “effectively trap-free” Estimate the trap-filled-limit voltage from the kink; in the simplest model Eq. (12).

$$V_{TFL} = \frac{eN_tL^2}{2\varepsilon} \tag{12}$$

which also gives the trap density N_t and then apply Mott-Gurney only to the high-voltage region well above the kink, but replace V with the excess bias (V_{TFL}) Eq. (13):

$$J = \frac{9}{8}\,\varepsilon_r\varepsilon_0\mu\,\frac{(V - V_{TFL})^2}{d^3} \tag{13}$$

From this concept, μ can be extracted exactly as in the trap-free case, and in this way, it is clear whether it really enters the post-TFL regime (the slope tends back to ~2 once the traps are filled). If the data never settles near 2 and instead maintains a super-quadratic slope, the culprit is often field-dependent mobility [33,34]. A very common description is

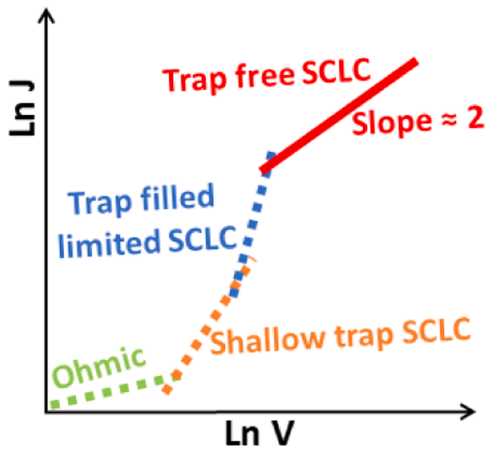

Fig. 1. The typical current-voltage scaling goes from the ohmic regime with low bias voltage to the shallow trap SCLC regime, the SCLC with trap filled limit, and finally the trap-free SCLC.

Poole-Frenkel- mobility, Eq. (14),

$$\mu(E) = \mu_0 \exp\left(\beta\sqrt{E}\right), \mathbf{E} = \frac{V}{d} \tag{14}$$

which leads to the Murgatroyd expression for SCLC (Eq. (15)),

$$J = \frac{9}{8}\,\varepsilon_r\varepsilon_0\mu_0\,\frac{V^2}{d^3}\,\exp\left(0.891\beta\sqrt{\frac{V}{d}}\right) \tag{15}$$

In practice, ln $(\frac{J}{V^2})$ is plotted against $\sqrt{\frac{V}{d}}$. The slope gives 0.891 β, and the intercept gives μ_0. In this way, it can specify both a zero-field mobility and its field activation parameter, which corresponds to real organic films much better than forcing a trap-free fit [35,36]. There is also the exponential of trap (Mark-Helfrich), in which an exponential trap distribution results in $J \propto V^{m+1}$ with $m = \frac{T_t}{T}$. The logarithmic slope immediately gives m, from which the characteristic trap temperature T_t can be derived. Mobility extraction in this model is possible but highly model-dependent; most researchers still combine this with a TFL analysis (for N_t) or proceed to Murgatroyd fitting to obtain μ_0 robustly [37, 38]. If the slope is < 2, it is not in the classical trap-free SCLC regime, so the simple Mott-Gurney extraction is not valid. Either fix the cause of the sub-square slope and then use Mott-Gurney, or switch to a different model/technique.

3.3. Device structures for the application of the SCLC technique

SCLC measurements intentionally use devices that contain only holes or only electrons, since Mott-Gurney's law only applies to the transport of a single carrier. When both holes and electrons are injected, the measured current no longer originates from only one type of charge moving under space charge confinement, but recombination occurs in the bulk, charge balance effects and possibly different mobilities for the two carriers [39]. This breaks through the simple physics behind SCLC. It should be noted that in this technique, single-carrier devices should be designed since the goal is to measure only one type of carrier mobility (either holes or electrons) without interference from the opposite carriers or additional recombination effects. If the device has multiple active layers or a blend of different materials, both electrons and holes might be injected and transported. This would lead to recombination, causing the J-V curve to deviate from the ideal SCLC model. Furthermore, according to the Mott-Gurney law for trap-free SCLCs, only one layer of uniform material with constant permittivity ε and mobility μ can be considered [40]. In the previous example [ITO/-TAPC/compound/TAPC/Al], both the anode side (ITO + TAPC) and the cathode side (Au + TAPC) are energetically aligned with the highest occupied molecular orbital (HOMO) of the tested compound, enabling efficient hole injection from both electrodes. This ensures that no electrons are injected, so that the measured current originates exclusively from holes. In addition, the use of TAPC ensures symmetrical contacts on both sides, avoiding differences in injection efficiency between the two electrodes. If the transport layers were different, one side could limit the injection due to an energy barrier, which would make the current injection- limited rather than space charge limited. In addition, the same hole transport layer (TAPC) creates a uniform electric field over the active layer on both sides, so that the assumptions of Mott-Gurney's law are more valid. This also allows a fair comparison of different compounds under identical injection conditions. When selecting adjacent materials, it should be considered that the HOMO of the hole transport layer (HTL) should be close to (or slightly above) the HOMO of the test compound and close to the anode work function (ITO/MoO_3, Au, etc.). As a rule of thumb, the barrier for the hole entry should be $\lesssim \sim 0.3$ eV. In contrast, choose an HTL with a high LUMO (large gap) so its LUMO sits well above the compound's LUMO, this suppresses electron injection and helps maintain a true hole-only current. A sizable LUMO offset ($\geq \sim 0.5$ eV is a good target) ensures that electrons do not escape from the opposite electrode into the HTL/compound, which would spoil the SCLC regime and bend the log J-log V slope away from 2 [41,42]. Taking into account, keep the HTL layers thin enough to avoid big series resistance but continuous to eliminate pinholes (often 10–30 nm works). Use the same HTL on both sides (e.g., ITO/TAPC/compound/TAPC/Al) so contacts are symmetric and the internal field is closer to uniform. Use high work function anodes (ITO with a thin MoO_3, or Au) to minimize the hole barrier, and avoid low work function cathodes that could inject electrons. Au as the counter electrode is common in hole-only stacks (Fig. 2**-a**). Upon biasing (ITO positive, Al negative), holes are readily injected from ITO into TAPC and then into the compound layer. At the opposite contact, the TAPC/Al interface, because of energy-level mismatch effectively blocks electron injection and is non- ohmic for holes, so the device behaves essentially as hole-only. The injected holes drift through the compound layer, but in the absence of compensating electrons they partially accumulate, building a positive space- charge density (Fig. 2**-b**). This space charge distorts the internal electric field weakening it near the cathode and strengthening it near the anode and thereby limits the current itself, i.e., SCLC. If traps are present, holes are initially captured and the current is low (injection/ohmic regime). As the voltage increases, the traps become filled and the I-V slope increases sharply at the trap-filled limit (TFL). In fact, with applying the voltage, 5 happens can be occurred [43–48]; 1) Starting the process (connecting the voltage source); ITO acts as the positive electrode (anode) and Al as the negative electrode (cathode), and the applied voltage shifts the energy levels on both sides relative to each other. 2) Hole injection from the ITO into the TAPC layer; since the HOMO of the TAPC is almost aligned with the work function of the ITO, holes are injected without a significant barrier from ITO into TAPC. In addition, the holes then easily move from TAPC into the compound layer because their HOMO levels are close in energy. 3) Hole injection from the Al side; Al is typically good for electron injection, but the TAPC layer in front of it has a high LUMO that blocks electrons from entering. Instead, holes are injected from Al into TAPC (with a small or moderate barrier), especially when the applied electric field assists this process at higher voltages. 4) Single-carrier (hole-only) current; because the high LUMO of TAPC blocks electron injection, the total current is carried entirely by holes traveling through the compound layer when the holes are injected from both sides, but the anode side usually has stronger injection. 5) SCLC regime; at higher voltages, a large number of holes are injected into the compound layer, and the internal electric field is modified by the accumulated charges. This is the SCLC regime, where the current follows the Mott-Gurney law, and in this condition, the current is no longer injection-limited but is controlled by the charge transport capacity of the material.

3.4. Practical example

In this study, a carbazole-containing dye was selected as an example; its chemical structure is provided in Fig. 3 [49].

3.4.1. Calculation carrier mobility by SCLC technique

According to the above explanation, first of all the fabricate hole only and electron only devices was done by solution process for active layer (compound) and physical vapor deposition (PVD) to deposited Al and LiF/Al as well. Due to the interpretation of previous section, the devices structures are illustrated in Fig. 4. The impressive notice is using lithium fluoride (LiF), when Al is evaporated onto an ultrathin LiF layer (≈0.5–1.0 nm), a strong interfacial dipole (and interfacial chemistry) is formed at the interface, which lowers the effective work function of Al and drastically reduces the barrier for electron entry into the organic LUMO. The cathode becomes nearly ohmic to electrons, so that the current is governed by the space charge in the bulk rather than by injection across a Schottky barrier. In this state, after the traps are filled, the device exhibits Mott-Gurney behaviour (J α $\frac{V^2}{d^3}$), from which the

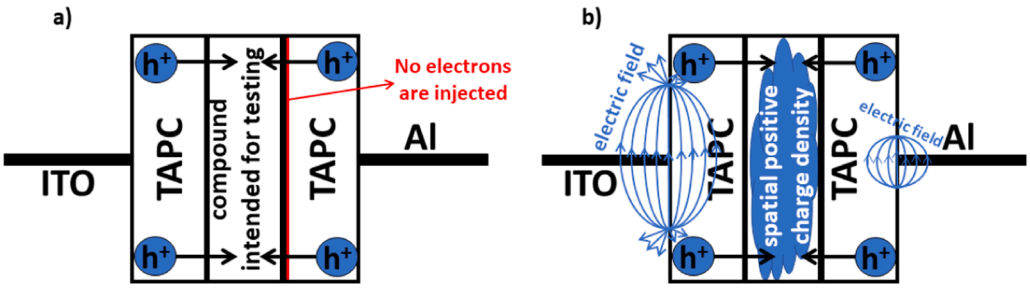

Fig. 2. (a) Schematic structure of the device and (b) representation of the small and large electric field.

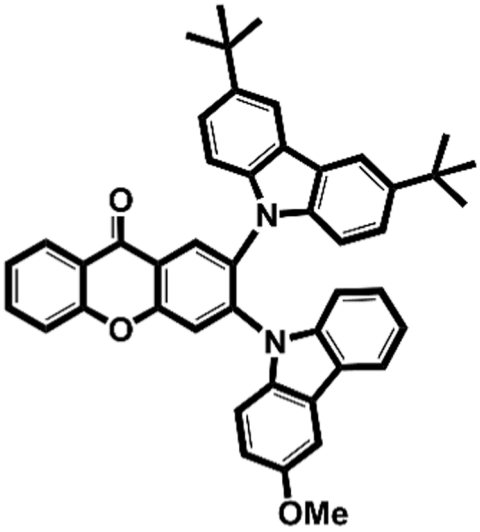

Fig. 3. The considered structure of compound.

electron mobility can be reliably derived [50]. Without LiF, Al often injects the electrons poorly into typical organic materials, the injection is contact-limited, the logJ-logV, slope deviates from ~2 (even after the trap-filled limit), and any mobility derived from this is not trustworthy, since the probing concerns the barrier, and not the bulk transport. It is worth mentioning that, LiF is not suitable for hole-only SCLC. At the LiF/Al contact, it lowers the work function and enhances electron injection, while providing a non-ohmic contact for holes. The current becomes injection-limited and bipolar, the J α V^2 regime is distorted, and the extracted hole mobility (μ_h) is unreliable [24,12,51]. The current-voltage characteristics of the electron-only and hole-only devices are shown in Fig. 5**-a** and **b**, respectively. Following the standard SCLC procedure, both axes were transformed using natural logarithms (Ln J versus Ln V), as presented in Fig. 6. The voltage region exhibiting a slope of approximately 2 was identified (Fig. 7), and linear fits were applied to this region (Fig. 8). The corresponding linear equations for the slope-2 region are reported in Fig. 9 as Ln J = 2.05 Ln V − 6.51 for the electron-only device and Ln J = 2.11 Ln V − 2.69 for the hole-only device, with slopes close to the ideal SCLC value of 2. Using these intercepts (−6.51 and −2.69) together with Eq. (11), the carrier mobilities were subsequently extracted.

$$J = \frac{9}{8}\,\varepsilon_r\varepsilon_0\mu\,\frac{V^2}{d^3} \text{ or } J = \frac{9}{8}\,\frac{\varepsilon_r\varepsilon_0}{d^3}\,\mu\,V^2$$

as $\frac{9}{8}\frac{\varepsilon_r\varepsilon_0}{d^3}$ and d = 200 nm = 2 × 10^{-5} cm, also ε_r~3 (ε_r~3 is a widely accepted and literature-supported value for π-conjugated organic compounds such as carbazole derivatives, and is commonly used in SCLC benchmarking studies [52–54]), and ε_0=8.854 × 10^{-14} F/cm, therefore,

$J = 37.33\,\mu V^2$ with using Ln in both side, Ln J= Ln 37.33+ Ln μ + Ln V^2 ➞

Ln J= Ln 37.33+ Ln μ + 2 Ln V ➞ Ln J = 2 Ln V + (Ln μ + Ln 37.33), therefore, the slope is 2 and intercept is (Ln μ + Ln 37.33), taking into account Fig. 9, (Ln μ + Ln 37.33) = −6.51 for electron device and (Ln μ + Ln 37.33) = −2.69 for hole device respectively.

For electron device; (Ln μ_e + Ln 37.33) = −6.51 ➞ (Ln μ_e + 3.61) = −6.51 ➞ Ln μ_e= −10.12, with using exp;

$$\mu_e = \exp(-10.12) \Rightarrow \mu_e = 4.02 \times 10^{-5} cm^2 v^{-1} s^{-1}$$

and

For hole device; (Ln μ_h + Ln 37.33) = −2.69 ➞ (Ln μ_h + 3.61) = −2.69 ➞ Ln μ_h= −6.30, with using exp;

$$\mu_h = \exp(-6.30) \Rightarrow \mu_h = 1.84 \times 10^{-3} \mathbf{cm}^2 v^{-1} s^{-1}$$

4. Conclusions

In this study, hole-only and electron-only devices based on a carbazole-containing compound were fabricated, enabling direct measurement of single-carrier transport under SCLC conditions. The experimental J-V characteristics revealed clear trap-free SCLC behavior (slope

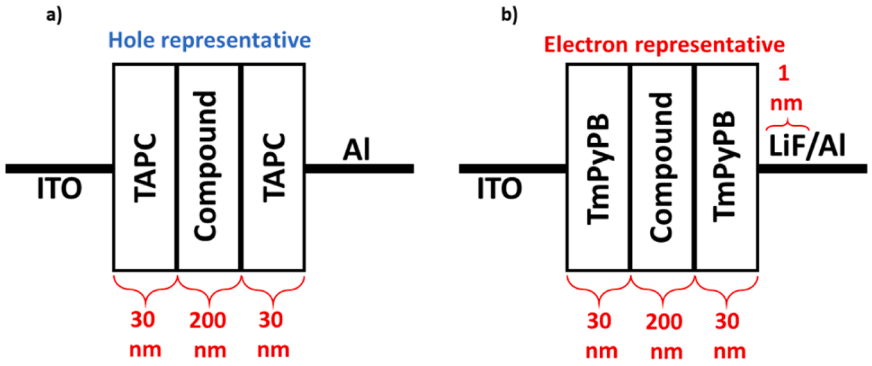

Fig. 4. The devices structures of (a) hole only and (b) electron only.

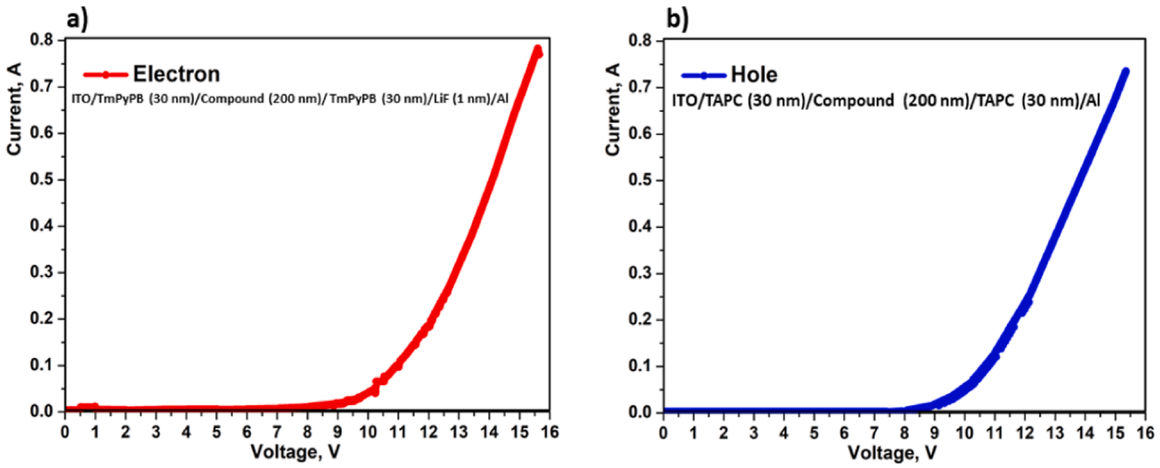

Fig. 5. Plot of voltage (V) vs current (J) for (a) electron and (b) hole based on the SCLC technique.

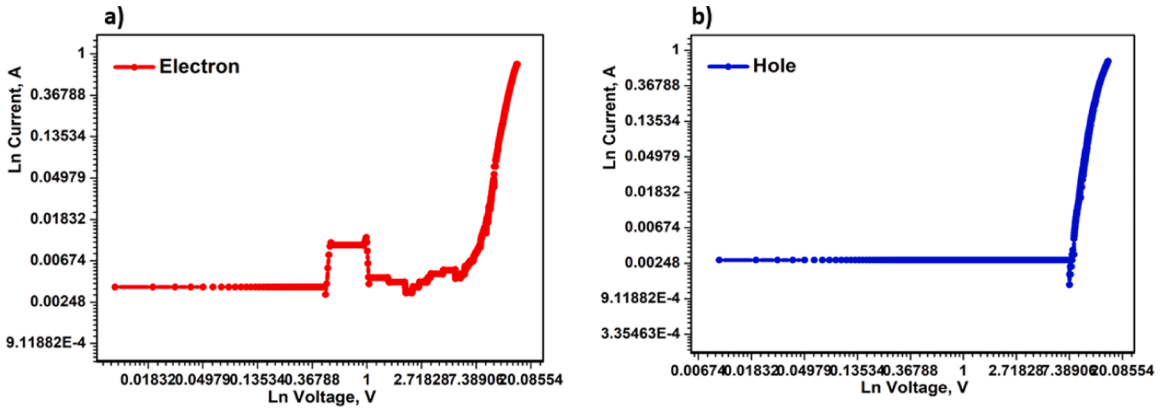

Fig. 6. Plot of Ln voltage (V) vs Ln current (J) for (a) electron and (b) hole based on the SCLC technique.

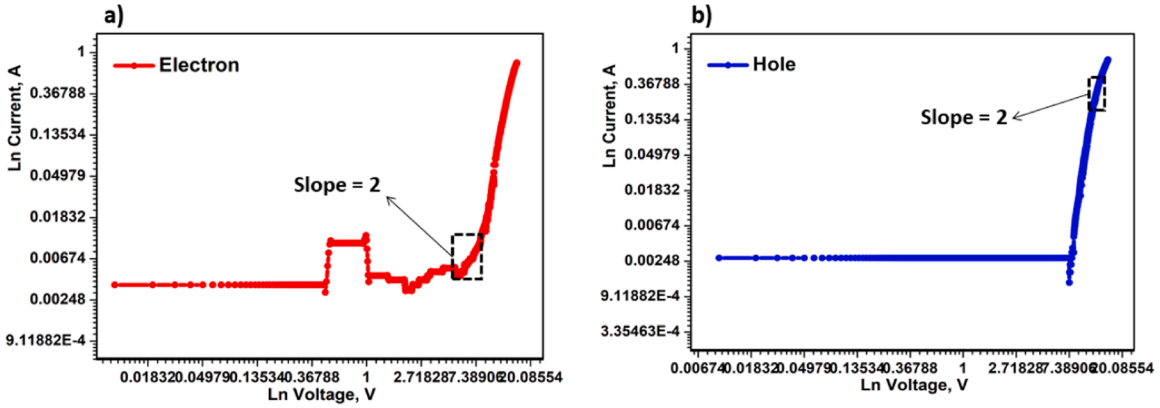

Fig. 7. The recognizing part of the plots J α V^2 (slope ~ 2) for (a) calculating electron mobility and (b) calculating hole mobility.

≈ 2), yielding mobilities of $\mu_e = 4.02 \times 10^{-5}$ cm^2 V^{-1} s^{-1} and $\mu_h = 1.84 \times 10^{-3}$ cm^2 V^{-1} s^{-1}, confirming strongly unbalanced charge transport in this material. These values are consistent with typical ranges reported for π-conjugated organic semiconductors and demonstrate the relevance of SCLC evaluation for assessing device-like transport performance. This work highlights the practical usefulness of SCLC for mobility extraction using simple device structures; however, it also acknowledges limitations such as the assumption of a constant dielectric, sensitivity to contact quality, and the requirement for well-defined single-carrier injection. Future work should include controlled-atmosphere measurements, repeated device batches, and comparison with complementary techniques such as TOF to further validate the mobility values.

Data availability

The data that has been used is confidential.

CRediT authorship contribution statement

Marzieh Rabiei: Visualization, Methodology, Investigation, Formal

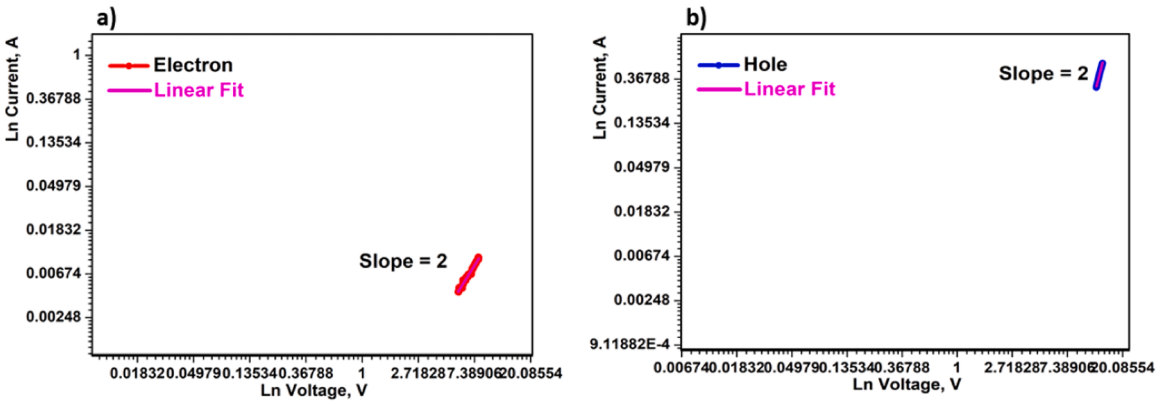

Fig. 8. Linear fit of the diagrams J α V^2 to prof (slope ~ 2) for (a) the calculation of the electron mobility and (b) the calculation of the hole mobility.

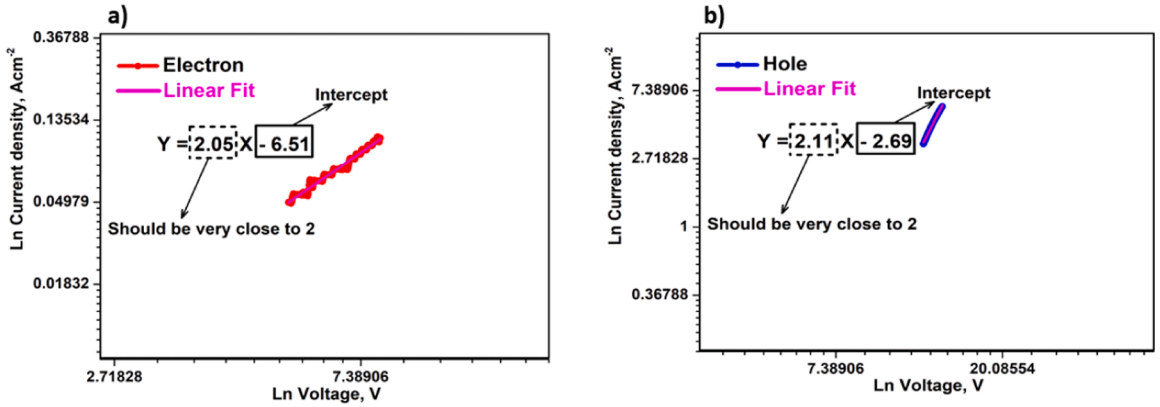

Fig. 9. Obtaining the equation of the line in (a) the calculation of the electron mobility and (b) the calculation of the hole mobility.

analysis, Data curation. **Sohrab Nasiri:** Writing – original draft, Software, Investigation. **Juozas Padgurskas:** Writing – review & editing, Validation, Supervision. **Raimundas Rukuiza:** Writing – review & editing, Visualization, Validation, Supervision.

Declaration of competing interest

The authors declare that they have no known competing financial interests or personal relationships that could have appeared to influence the work reported in this paper.

Acknowledgments

This project has received funding from the Research Council of Lithuania (LMTLT), agreement No S-PD-24–82.

References

[1] Hall Mobility of Holes in Silver Bromide - Roland Clements Hanson - Google Books, (n.d.). https://books.google.ca/books/about/Hall_Mobility_of_Holes_in_Silver_Bromide.html?id=McfHQMopLSQC&redir_esc=y (accessed August 14, 2025).
[2] G. Mascali, V. Romano, J.M. Sellier, Hole mobility in silicon semiconductors, (2006) 363–368. https://doi.org/10.1007/978-3-540-32862-9_52.
[3] C. Tanase, P.W.M. Blom, D.M. de Leeuw, E.J. Meijer, Charge carrier density dependence of the hole mobility in poly(p-phenylene vinylene), Phys. Org. Semicond. (2006) 305–318, https://doi.org/10.1002/3527606637.CH11.
[4] C.E. Armentrout, The Hall effect in copper: an undergraduate experiment, Am. J. Phys. 58 (1990) 758–762, https://doi.org/10.1119/1.16379.
[5] J. Lim, M. Kober-Czerny, Y.H. Lin, J.M. Ball, N. Sakai, E.A. Duijnstee, M.J. Hong, J. G. Labram, B. Wenger, H.J. Snaith, Long-range charge carrier mobility in metal halide perovskite thin-films and single crystals via transient photo-conductivity, Nat. Commun. 13 (2022) 1–9, https://doi.org/10.1038/s41467-022-31569-w, 2022 13:1.
[6] S. Seki, A. Saeki, T. Sakurai, D. Sakamaki, Charge carrier mobility in organic molecular materials probed by electromagnetic waves, Phys. Chem. Chem. Phys. 16 (2014) 11093–11113, https://doi.org/10.1039/C4CP00473F.
[7] K. Sebastian Radke, F. Ortmann, G. Cuniberti, Concepts and modeling for charge transport in organic electronic materials, RSC Smart Mater. (2014) 273–308, https://doi.org/10.1039/9781782626947-00273, 2015-January.
[8] P. Bhaskar, A.W. Achtstein, S.L. Diedenhofen, L.D.A. Siebbeles, Mobility and decay dynamics of charge carriers in one-dimensional selenium van der Waals solid, J. Phys. Chem. C 121 (2017) 18917–18921, https://doi.org/10.1021/ACS.JPCC.7B05183/ASSET/IMAGES/LARGE/JP-2017-051836_0003.JPEG.
[9] R. Brüggemann, G.H. Bauer, Identification and explanation of peculiar features in hole SCLC-TOF in a-Si:h pin-diodes from numerical modelling, J. Non. Cryst. Solids. 198-200 (1996) 186–189, https://doi.org/10.1016/0022-3093(95)00678-8.
[10] R. Brueggemann, G.H. Bauer, Numerical modelling of time-of-flight in SCLC-mode, in: Materials Research Society Symposium - Proceedings 377, 1995, pp. 497–502, https://doi.org/10.1557/PROC-377-497/METRICS.
[11] S.W. Liu, C.C. Lee, W.C. Su, C.H. Yuan, C.F. Lin, K.T. Chen, Y.S. Shu, Y.Z. Li, T. H. Su, B.Y. Huang, W.C. Chang, Y.H. Liu, Downscaling the sample thickness to sub-micrometers by employing organic photovoltaic materials as a charge-generation layer in the time-of-flight measurement, Sci. Rep. 5 (2015) 1–15, https://doi.org/10.1038/srep10384, 2015 5:1.
[12] D. Jiang, J. Sun, R. Ma, V.K. Wong, J. Yuan, K. Gao, F. Chen, S.K. So, X. Hao, G. Li, H. Yin, Extracting charge carrier mobility in organic solar cells through space-charge-limited current measurements, Mater. Sci. Eng.: R: Rep. 157 (2024) 100772, https://doi.org/10.1016/J.MSER.2024.100772.
[13] Y. Li, R.G. Clevenger, L. Jin, K.V. Kilway, Z. Peng, Unusually high SCLC hole mobility in solution-processed thin films of a polycyclic thiophene-based small-molecule semiconductor, J. Mater. Chem. C. Mater. 2 (2014) 7180–7183, https://doi.org/10.1039/C4TC01181C.
[14] J. De, R. De, I. Bala, S.P. Gupta, R.S. Yadav, U.K. Pandey, S.K. Pal, Molecular design and alignment for ambipolar SCLC mobility in self-assembled columnar discogens, Small. Methods 9 (2025) 2401634, https://doi.org/10.1002/SMTD.202401634.
[15] S. Dahlström, C. Ahläng, K. Björkström, S. Forsblom, B. Granroth, K. Jansson, A. Luukkonen, M.T. Masood, J. Poulizac, S. Qudsia, M. Nyman, Extraction current transients for mobility determination-A comparative study, AIP. Adv. 10 (2020) 65203, https://doi.org/10.1063/5.0008802/993830.
[16] M. Funahashi, Time-of-flight method for determining the drift mobility in organic semiconductors, Org. Semicond. Optoelectron. (2021) 161–178, https://doi.org/10.1002/9781119146131.CH6.

[17] J. Urbančič, E. Tomsič, M. Chhikara, N. Pastukhova, V. Tkachuk, A. Dixon, A. Mavrič, P. Hashemi, D. Sabaghi, A.S. Nia, G. Bratina, E. Pavlica, Time-of-flight photoconductivity investigation of high charge carrier mobility in Ti3C2Tx MXenes thin-film, Diam. Relat. Mater. 135 (2023) 109879, https://doi.org/10.1016/J.DIAMOND.2023.109879.
[18] F. Neumann, Y.A. Genenko, R. Schmechel, H. Von Seggern, Role of diffusion on SCLC transport in double injection devices, Synth. Met. 150 (2005) 291–296, https://doi.org/10.1016/J.SYNTHMET.2005.03.005.
[19] A.L. Garner, N.R.S. Harsha, A.M. Loveless, Extending the Mott-Gurney law to one-dimensional nonplanar diodes using point transformations, J. Appl. Phys. 137 (2025), https://doi.org/10.1063/5.0276418.
[20] W. Chandra, L.K. Ang, K.L. Pey, C.M. Ng, Two-dimensional analytical Mott-Gurney law for a trap-filled solid, Appl. Phys. Lett. 90 (2007), https://doi.org/10.1063/1.2721382/166699.
[21] A.R. Buckley, Analysing space charge limited currents in organic light emitting diodes, Synth. Met. 160 (2010) 540–543, https://doi.org/10.1016/J.SYNTHMET.2009.11.027.
[22] M. Giulianini, E.R. Waclawik, J.M. Bell, N. Motta, Current-voltage characteristics of poly(3-hexylthiophene) diodes at room temperature, Appl. Phys. Lett. 94 (2009), https://doi.org/10.1063/1.3086882/337522.
[23] A. Pitarch, K. Meerholz, D. Hertel, Effect of dopant concentration on charge transport in crosslinkable polymers, Phys Status Solidi B Basic Res 245 (2008) 814–819, https://doi.org/10.1002/PSSB.200743457;REQUESTEDJOURNAL:JOURNAL:15213951;WGROUP:STRING:PUBLICATION.
[24] S. Arya, P. Mahajan, R. Gupta, R. Srivastava, N. kumar Tailor, S. Satapathi, R. R. Sumathi, R. Datt, V. Gupta, A comprehensive review on synthesis and applications of single crystal perovskite halides, Prog. Solid State Chem. 60 (2020) 100286, https://doi.org/10.1016/J.PROGSOLIDSTCHEM.2020.100286.
[25] M.J. Sharifi, F.A. Gooraji, A quantitative index for injection/transport mechanism in organic light-emitting diodes, J. Org. Semicond. 1 (2013) 1–6, https://doi.org/10.1080/21606099.2013.771505.
[26] M. Sajedi Alvar, P.W.M. Blom, G.J.A.H. Wetzelaer, Space-charge-limited electron and hole currents in hybrid organic-inorganic perovskites, Nat. Commun. 11 (2020) 1–9, https://doi.org/10.1038/s41467-020-17868-0, 2020 11:1.
[27] K. Sivula, Improving charge carrier mobility estimations when using space-charge-limited current measurements, ACS. Energy Lett. 7 (2022) 2102–2104, https://doi.org/10.1021/ACSENERGYLETT.2C01154/ASSET/IMAGES/LARGE/NZ2C01154_M002.JPEG.
[28] A. Kokil, K. Yang, J. Kumar, Techniques for characterization of charge carrier mobility in organic semiconductors, J. Polym. Sci. B Polym. Phys. 50 (2012) 1130–1144, https://doi.org/10.1002/POLB.23103.
[29] J.C. Blakesley, F.A. Castro, W. Kylberg, G.F.A. Dibb, C. Arantes, R. Valaski, M. Cremona, J.S. Kim, J.S. Kim, Towards reliable charge-mobility benchmark measurements for organic semiconductors, Org. Electron. 15 (2014) 1263–1272, https://doi.org/10.1016/J.ORGEL.2014.02.008.
[30] S. Gavranovic, O. Zmeskal, M. Weiter, J. Pospisil, Advanced space-charge-limited current model for analyzing fermi level shift in the bandgap of halide perovskites, Commun. Phys. 8 (2025) 1–10, https://doi.org/10.1038/S42005-025-02202-1;SUBJMETA=1005,301,4062,4072,4077,639,766;KWRD=DEVICES+FOR+ENERGY+HARVESTING,MATERIALS+FOR+DEVICES,MATERIALS+SCIENCE,PHYSICS.
[31] Z.B. Wang, M.G. Helander, M.T. Greiner, J. Qiu, Z.H. Lu, Carrier mobility of organic semiconductors based on current-voltage characteristics, J. Appl. Phys. 107 (2010), https://doi.org/10.1063/1.3305341/913807.
[32] T. Yasuda, Y. Yamaguchi, D.C. Zou, T. Tsutsui, Carrier mobilities in organic electron transport materials determined from space charge limited current, Jpn. J. Appl. Phys. 1: Regul. Pap. Short Notes Rev. Pap. 41 (2002) 5626–5629, https://doi.org/10.1143/JJAP.41.5626/XML.
[33] S. Tiwari, N.C. Greenham, Charge mobility measurement techniques in organic semiconductors, Opt. Quantum. Electron. 41 (2009) 69–89, https://doi.org/10.1007/S11082-009-9323-0/METRICS.
[34] S. Nasiri, P. Palanisamy, M. Rabiei, M. Hosseinnezhad, A. Palevicius, A. Vilkauskas, G. Janusas, V. Nutalapati, Investigation of the influence of persulfurated benzene derivatives on optical and carrier mobility properties, Mater. Lett. 342 (2023) 134323, https://doi.org/10.1016/J.MATLET.2023.134323.
[35] K. Alkhezaim, Charge carrier mobility of non-fullerene acceptors in single-carrier electron-only devices, (2024).
[36] S. Dahlström, C. Ahläng, K. Björkström, S. Forsblom, B. Granroth, K. Jansson, A. Luukkonen, M.T. Masood, J. Poulizac, S. Qudsia, M. Nyman, Extraction current transients for mobility determination-A comparative study, AIP. Adv. 10 (2020) 65203, https://doi.org/10.1063/5.0008802/993830.
[37] M.M. Mandoc, B. de Boer, G. Paasch, P.W.M. Blom, Trap-limited electron transport in disordered semiconducting polymers, Phys. Rev. B 75 (2007) 193202, https://doi.org/10.1103/PhysRevB.75.193202.
[38] X. Hu, H. Wang, M. Wang, Z. Zang, Interfacial defects passivation using fullerene-polymer mixing layer for planar-structure perovskite solar cells with negligible hysteresis, Sol. Energy 206 (2020) 816–825, https://doi.org/10.1016/J.SOLENER.2020.06.057.
[39] V.M. Le Corre, E.A. Duijnstee, O. El Tambouli, J.M. Ball, H.J. Snaith, J. Lim, L.J. A. Koster, Revealing charge carrier mobility and defect densities in metal halide perovskites via space-charge-limited current measurements, ACS. Energy Lett. 6 (2021) 1087–1094, https://doi.org/10.1021/ACSENERGYLETT.0C02599/ASSET/IMAGES/MEDIUM/NZ0C02599_M005.GIF.
[40] Z.B. Wang, M.G. Helander, M.T. Greiner, J. Qiu, Z.H. Lu, Carrier mobility of organic semiconductors based on current-voltage characteristics, J. Appl. Phys. 107 (2010) 34506, https://doi.org/10.1063/1.3305341/913807.
[41] A.R. Tameev, A.E. Aleksandrov, I.R. Sayarov, S.I. Pozin, D.A. Lypenko, A. V. Dmitriev, N.V. Nekrasova, A.Y. Chernyadyev, A.Y. Tsivadze, Charge carrier mobility in poly(N,N′-bis-4-butylphenyl-N,N′-bisphenyl)benzidine composites with electron acceptor molecules, Polym. (Basel) 16 (2024) 570, https://doi.org/10.3390/POLYM16050570, 2024, Vol. 16, Page 570.
[42] H. Wang, M. Bruna, P. Olivero, S. Borini, F. Picollo, O. Budnyk, F. Bosia, Ž. Pastuovic, N. Skukan, M. Jakšič, E. Vittone, Space charge limited current (SCLC) as observed on diamond surface damaged by MeV ion implantation, IOP. Conf. Ser. Mater. Sci. Eng. 16 (2010) 012004, https://doi.org/10.1088/1757-899X/16/1/012004.
[43] J. Dacuña, A. Salleo, Modeling space-charge-limited currents in organic semiconductors: extracting trap density and mobility, Phys. Rev. B Condens. Matter. Mater. Phys. 84 (2011) 195209, https://doi.org/10.1103/PHYSREVB.84.195209/FIGURES/12/THUMBNAIL.
[44] M. Zubair, Y.S. Ang, L.K. Ang, Thickness dependence of space-charge-limited current in spatially disordered organic semiconductors, IEEe Trans. Electron. Devices 65 (2018) 3421–3429, https://doi.org/10.1109/TED.2018.2841920.
[45] J. Ko, M.M. Winslow, J. Sage, Mechanisms of small cell lung cancer metastasis, EMBo Mol. Med. 13 (2021), https://doi.org/10.15252/EMMM.202013122/ASSET/7D955307-4527-4A6A-8EFF-9D11500A1444/ASSETS/GRAPHIC/EMMM202013122-FIG-0002-M.PNG.
[46] J.A. Röhr, X. Shi, S.A. Haque, T. Kirchartz, J. Nelson, Charge transport in Spiro-OMeTAD investigated through space-Charge-limited current measurements, Phys. Rev. Appl. 9 (2018) 044017, https://doi.org/10.1103/PHYSREVAPPLIED.9.044017/FIGURES/6/THUMBNAIL.
[47] G. Landi, A.V. Tunc, A. De Sio, J. Parisi, H.C. Neitzert, Hole-mobility limits for the Zn(OC)2 organic semiconductor obtained by SCLC and field-effect measurements, Phys. Status Solidi (a) 213 (2016) 1909–1914, https://doi.org/10.1002/PSSA.201532931.
[48] M. Nikolka, K. Broch, J. Armitage, D. Hanifi, P.J. Nowack, D. Venkateshvaran, A. Sadhanala, J. Saska, M. Mascal, S.H. Jung, J.K. Lee, I. McCulloch, A. Salleo, H. Sirringhaus, High-mobility, trap-free charge transport in conjugated polymer diodes, Nat. Commun. 10 (2019) 1–9, https://doi.org/10.1038/S41467-019-10188-Y;TECHMETA=128;SUBJMETA=1130,2798,301,3931,639,766,923;KWRD=ELECTRONIC+AND+SPINTRONIC+DEVICES,ORGANIC+MOLECULES+IN+MATERIALS+SCIENCE.
[49] S. Nasiri, A. Dashti, M. Hosseinnezhad, M. Rabiei, A. Palevicius, A. Doustmohammadi, G. Janusas, Mechanochromic and thermally activated delayed fluorescence dyes obtained from D-A-D′ type, consisted of xanthen and carbazole derivatives as an emitter layer in organic light emitting diodes, Chem. Eng. J. 430 (2022) 131877, https://doi.org/10.1016/J.CEJ.2021.131877.
[50] S. Nasiri, P. Palanisamy, M. Rabiei, M. Hosseinnezhad, A. Palevicius, A. Vilkauskas, G. Janusas, V. Nutalapati, Investigation of the influence of persulfurated benzene derivatives on optical and carrier mobility properties, Mater. Lett. 342 (2023) 134323, https://doi.org/10.1016/J.MATLET.2023.134323.
[51] M.P. Bracciale, C. Kim, A. Marrocchi, Organic electronics: an overview of key materials, processes, and devices, Sustainable Strategies in Organic Electronics (2022) 3–71. https://doi.org/10.1016/B978-0-12-823147-0.00001-X.
[52] Z. Li, D. Song, Z. Xu, B. Qiao, S. Zhao, S. Wageh, A.A. Al-Ghamdi, X. Huo, Synergetic effect of different carrier dynamics in Pm6:Y6:ITIC-M Ternary Cascade Energy Level System, Polym. (Basel) 13 (2021) 2398, https://doi.org/10.3390/polym13152398.
[53] F. Wu, S. Mabrouk, M. Han, Y. Tong, T. Zhang, Y. Zhang, R.S. Bobba, Q. Qiao, Effects of electron- and hole-current hysteresis on trap characterization in organo-inorganic halide perovskite, J. Energy Chem. 76 (2023) 414–420, https://doi.org/10.1016/j.jechem.2022.10.011.
[54] R.H. Bube, Trap density determination by space-charge-limited currents, J. Appl. Phys. 33 (1962) 1733–1737, https://doi.org/10.1063/1.1728818.